# Soluble salt deposit in the Nihewan beds and its environmental significance

LI Rongquan (李容全)[1], QIAO Jianguo (乔建国)[2], QIU Weili (邱维理)[1], ZHAI Qiumin (翟秋敏)[1] & LI Yongliang (李永良)[3]

1. Department of Resources and Environmental Science, Beijing Normal University, Beijing 100875, China;
2. Dean' s Office of Shanxi Normal University, Linfen 041004, China;
3. The Center for Analyses and Tests, Beijing Normal University, Beijing 100875, China
Correspondence should be addressed to Li Rongquan (email: geo@bnu.edu.cn)

Received June 9, 1999

**Abstract** Observation and experimental analysis of soluble salt deposit along four profiles across the strata deposited in Nihewan paleolake basin enabled us to recognize the nature and evolution stages of the Nihewan paleolake and its significance in stratigraphical division and paleo-environmental reconstruction. The Nihewan paleolake was at least a weak-saline to semi-saline lake and represents an intracontinental lake in the semi-arid region. The lower member of sedimentary strata in the paleolake contains gypsum layer and gypsum lamellae. Soluble salt is mainly composed of $SO_4^{2-}$ and $Ca^{2+}$ ions, representing a trend of the paleolake evolving into a stage of sulfate lake. The upper member of the strata has predominantly $Cl^-$, $K^+$, and $Na^+$ ions in soluble salt, indicating a starting development of the paleolake to chlorite lake, but no salt rock was deposited, indicating a drying trend of the area.

**Keywords:** **Nihewan beds, soluble salt deposit, paleo-environment, semi-saline lake.**

## 1 Present status of research on Nihewan paleolake

Since the fluvial-lacustrine deposits found in the area nearby Nihewan Village in Yangyuan County, Hebei, was named "Nihowan Beds" by Barbour[1], they have attracted the attention of archaeologists and geologists because of their wide distribution and abundant mammal fossils in them and became well known in the world. Before the 1940s the researches into the Nihewan beds were in the following three aspects: (i) Systematic stratigraphic division of the beds exposed in the eastern part of the basin in ascending order: lateritic bed, gravel and sand layers, sandy soil layer, and white marl[2]; (ii) study of large amount of mammal fauna in the beds, which were named Nihewan fauna[3]; (iii) according to the faunal characteristics the lateritic bed was identified as a Pliocene deposit and the other three beds correspond to the Villafranchian deposit in Europe[2] and to the deposit of Sanmen epoch[4]. Based on the principle of Tertiary-Quaternary boundary division adopted at the 18th session of International Geological Congress in 1948, the Nihewan Beds were determined to be the early Pleistocene marker deposit in North China by Chinese geologists after 1949[5].

A paleolith was found in sand layer nearby Nihewan Village by Gai and Wei in 1972[6]. Since

then a new chapter on studies of paleoanthropological fossils and paleolithic traces in Nihewan area was started. The well-known traces are the late Pleistocene Xujiayao Trace with paleoanthropological and mammal fossils and paleoliths[7] and the Xiaochangliang Paleolithic Trace to be dated[8]. A lot of the micropaleontological research results of Nihewan area was published in the 1970s and 1980s. Based on their study on foraminifera fossils, Huang and Guo suggested that during accumulation of the middle and upper members of Nihewan beds the paleolake was weakly saline or semi-saline[9]. By their paleomagnetic study Cheng et al. suggested that the Nihewan beds at Xiaodukou were accumulated in between 3 Ma BP and 1.6 Ma BP[10]. Later, Li and Wang believed that the Nihewan beds were deposited in 3.1 Ma B.P.—0.3 or 0.2 Ma BP[11]. Since the 1990s, Li and Yuan first described the Pleistocene stromatolith in the top section of Hutouliang profile[12]. Xia et al. have identified algae fossils found in two stromatolithic layers at the same site and dated their survival time to be $9.4\times10^4$ a BP and $13.2\times10^4$ a BP[13]. Yuan et al. have divided the Nihewan beds into three members by using their integrated stratigraphic division method: member I was dated to be 3.40—2.48 Ma BP by using paleomagnetic method, member II to be 2.48—0.97 Ma BP, and member III to be 0.97—0.13 Ma BP. Thus, a new stratigraphical framework of the Nihewan Formation was established[14].

In addition to the studies described above, the neotectonic movement of the basin was also studied in the 1950s[15, 16], and the Cenozoic deposits in the basin were studied from paleogeography[17] and systematic stratigraphy[18]. But problems of the characteristics of soluble salt in the Nihewan beds, the nature, development, and evolution of the paleolake, which the soluble salt can reflect, and its environmental characteristics, remain to be further studied.

## 2 Observation on stratigraphic profiles

For systemic observation on the soluble salt deposit and its distribution in the Nihewan beds and comparison between the soluble salt deposits in lake-shore zone and central lake zone, we have selected the Jingerwa and Hutouliang-Xueergou profiles, which represent the deposit in central lake zone, and the northern Shuiquan-Pulu and Hongya-Nangou profiles which represent the deposit in lake-shore zone. Here only the characteristics of Xueergou and Hongya profiles are described.

### 2.1 The Hutouliang-Xueergou profile

The deposit exposed along the profile is 70 m thick and its bottom is occupied by a reservoir. It is actually 55.7 m thick along the profile and its lithological characteristics will be described in descending order as follows:

Upper Member

17. Malan loess bed. 0.3 m
16. Yellow to yellow-gray breccia with calcareous cement, which represents siliceous limestone, of deluvial deposit. 0.5 m
15. Gravel-mixing clayey soil in upper part and gray-green silt and gravel in lower part. 1.3 m

14. Grayish gravel layer. The gravel is mainly of dolomite limestone, 98%, and less of Jurassic purple shale. No basalt gravel was found. Highly rounded and flattened gravels are 1/2—1/3; coarse and larger gravels (5—8 cm) are angular. The gravels are covered with calcium carbonate and have isoclinal bedding. 1.3 m
13. Yellow to gray-green silt and clayey soil interlayers, with a thin fine-grained sand layer. 1.1 m
12. Gray-green silt and clayey soil interlayers, with a thin gravel layer at the bottom. 1 m
11. Brown-yellow clayey soil in upper part and gray-green silt in lower part. This layer changes gradually eastward into a gravel layer, with calcretes at the top and bottom, respectively. 0.6 m
10. Gray gravel layer. The gravel is covered with a small amount of calcium carbonate. 1.3 m
9. Yellow silt and gray-green clayey soil and clay interlayers, with calcrete near the bottom. 2.4 m
8. Gray-green to dark-gray-green clay, intercalating thin silt and fine-grained sand layers, with two calcretes at the bottom. 5.8 m
7. Yellow silt and fine-grained sand layer, having wave ripple and near-horizontal bedding, with cross-bedding on the top surface. 4.5 m

Lower Member

6. Gravel layer, having tabular-isoclinal bedding. The gravel has high roundness and sphericity and is composed of siliceous limestone and Jurassic volcanic rock. Not basalt was found. 1 m below the top surface, many transparent gypsum crystals are scattered on the outcrop surface. Calcrete occurs at the bottom. 4 m
5. Gray-yellow clay and thin yellow silt interlayers. 2.6 m
4. Silt layer, having cross-bedding. 0.5 m
3. Gray-yellow clay and thin yellow silt layer, having ribbon bedding. 6 gypsum lamellae occur 1.7 m below the top surface. 9.8 m
2. Gray-yellow to gray-green thin clay and silt interlayers, locally with silt lenses having cross-bedding. *Pungitius* fish fossil was found at the top of the layer. 6.3 m
1. Dark-gray-green clay, intercalating with thin silt layer. 11.4 m

## 2. 2 Hongya-Nangou profile

Deposit along the profile is 94.40 m thick; fluvial-lacustrine deposit is 90.26 m in total. Lithological characteristics of the deposit are described in descending order as follows:

Upper Member

43. Gravel layer, having isoclinal tabular bedding. A gray-green clayey soil layer at the bottom. 1.8 m
42. Gravel layer, having isoclinal tabular bedding. Gravels are covered with white calcium sediment. 4.1 m
41. Gray-green clayey soil. 0.92 m
40. Gray-green clayey soil and brown-yellow clayey soil interlayers. 1.2 m
39. Gray-green calcium silt and clayey soil interlayers. 1.17 m
38. Brown-yellow clayey soil. 0.9 m
37. Gray gravel layer, with calcrete at its top and bottom, respectively. 0.6 m
36. Orange-yellow clayey soil, intercalating two calcretes. 2.25 m
35. Gravel-containing coarse sand. 0.6 m
34. Gray-green silt and clayey soil interlayers. 1.5 m
33. Gravel layer, intercalating gray-green clayey soil and one calcrete. 3.1 m

32. Orange-yellow silt-fine-grained sand layer, with a 0.45-m-thick gravel layer at the bottom. 1.12 m
31. Gray-green silt, with gray-green clayey soil at the bottom and a calcrete at the base. 0.8 m
30. Gray clayey soil and silt interlayers. 1.0 m
29. Brown-yellow clayey soil. 0.8 m
28. Gray-green silt and clayey soil interlayers. 0.89 m
27. Brown-yellow clayey soil, with a calcrete at the bottom. 1.21 m
26. Gravel layer. 1.0 m
25. Brown-yellow silt layer, with calcretes in the middle and at the bottom, respectively. 4.0 m
24. Gray-green silt, intercalating brown-yellow clayey soil and clay layers, with a calcrete at the bottom. 3 m

Lower Member

23. Gray-green silt and brown-yellow clayey soil interlayers, with a calcrete at the bottom. 3.6 m
22. Gray-green silt layer, with a calcrete at the bottom. 0.8 m
21. Gray-green silt and clayey soil interlayers, with a calcrete at the bottom. 0.8 m
20. Gray-green silt, intercalating brown-yellow clay layer, with 3 calcretes. 2.15 m
19. Gravel layer. 0.5 m
18. Grayish calcic clayey soil, intercalating gravel layer, with a calcrete at the bottom. 1.75 m
17. Gray-green silt and clay interlayers, with a calcrete at the bottom. 0.4 m
16. Calcic clayey soil layer, intercalating thin gravel layer. 1.25 m
15. Gray-green and brown-yellow clayey soil interlayers, intercalating fine-grained gravel layer and 3 calcretes. 5.15 m
14. Gray-green clayey soil and yellow sandy soil interlayers, intercalating a 0.1-m-thick calcrete in the middle part. 7.7 m
13. Gravel layer, its 0.3-m-thick lower part has isoclinal bedding and 0.7-m-thick upper part has clear curling with amplitude of 0.4 m. 1.4 m
12. Gray-green clayey soil, silt, and sandy soil interlayers. 0.6 m
11. Gravel layer, intercalating grey-green silt layer. High flatness of the gravel; with calcrete at the bottom and top. 0.7 m
10. Silt-fine-grained sand interlayers, mainly silt. 1.0 m
9. Gray-green clayey soil and sandy soil interlayers, with yellow-brown clayey soil at the bottom. 4.8 m
8. Gravel layer. 2.1 m
7. Yellow-brown silt, becomes westward coarse, rock debris appears, and a calcrete in the top part. 6.9 m
6. Yellow-green to gray-green silt layer. 9.5 m
5. Gravel layer, with isoclinal tabular-oblique bedding. 1.6 m
4. Yellow-green to gray-green silt layer. 2.5 m
3. Gray clay layer, rich in mirabilite, with abundant snail fossil. 1.0 m
2. Yellow-brown to brown clay layer, containing *Lamprotula* fossils. The species are more complex than those deposits along the Pulu profile. The layer changes southeastward into black to gray-black silt layer. 2 m
1. Red clay layer ($N_2$), with gravel, lies in an erosional contact on andesitic conglomerate. 4.14 m

The lithological characteristics of deposit along the Jingerwa profile are similar to those

along Xueergou profile. There exists gypsum in the lower part along the profile and multi-layer calcretes in the upper part. Lithological characteristics of deposit along the Pulu profile are similar to those along Hongya-Nangou profile. At the base of both profiles, lake-shore swamp silt has evolved upward into lake-shore and lake deposits containing *Lamprotula*. The difference between them is that gypsum exists in the lower part along the Pulu profile and only mirabilite in the lower part along the Hongya profile. But they both are of sulfate deposit. Since there exists syngenetic soluble salt (sulfate minerals) in the lower part and carbonate (calcrete) in the upper part along the four profiles, a correlation between them can be preliminarily set up in field work. From the amount of main ions in soluble salt obtained in experiments and the characteristics of facies change, the deposit along the profiles can be divided into upper and lower members. The upper member is 0.80—21.10 m and the lower member is 21.10—55.70 m along the Xueergou profile, whereas the upper member is 0—32.06 m and the lower member is 32.06—90.26 m along the Hongya profile.

If the cumulative thickness ratios $(h_{g+s})/h_n=A$ and $h_l/h_n=L$ (table 1) are used in comparison between the upper and lower members along these four profiles, the *A* value for the lower member along the Pulu and Hongya profiles will be 0.32 and 0.55, respectively, reflecting the lake-shore sedimentary characteristics. This is coincident with that the sites of the two profiles are close to mountains and bedrock on the lake basin margin and the regularity of lake deposit, the thickness of which is larger than that in shallow lake zone, as no significant local differential-tectonic movement occurred at the same erosional datum. For the lower member along the Xueergou profile, $A$=0.13, indicating the effect of geological process on it was less than that along the Pulu and Hongya profiles. The Jingerwa profile lies just in a shallow lake zone.

Table 1 Comparison between *A* and *L* values along four profiles

| Name of profile | Hongya | | Pulu | | Xueergou | | Jingerwa | |
|---|---|---|---|---|---|---|---|---|
| | *A* | *L* | *A* | *L* | *A* | *L* | *A* | *L* |
| Upper member | 0.48 | 0.52 | 0.22 | 0.78 | 0.50 | 0.50 | 0.11 | 0.89 |
| Lower member | 0.55 | 0.45 | 0.32 | 0.68 | 0.13 | 0.87 | 0 | 1.0 |

$h_{g+s}$ is cumulative thickness of silt-fine-grained sand and gravel layers; $h_l$ is cumulative thickness of lacustrine deposit; $h_n$ is cumulative thickness of upper or lower member.

*A* value for the upper members along the Hongya and Pulu profiles decreases, but *L* value increases more sharply than that for the lower members. It may be caused by the uprise and extension of the lake surface. *A* value for the upper member along the Xueergou profile increases suddenly and *L* value decreases, indicating an uprise of the lake basin bottom along the Xueergou profile during deposition of the upper member, so that it was close to the lake shore or became a part of the shore. The upper member along Jingerwa profile has $A$=0.11, which may indicate the shallowing of the whole lake at that time (fig. 1(a)).

## 3 Microscopic observations

For examining the distribution of lower members along the Xueergou and Jinerwa profiles, we performed short-distance photography and analyses of the sediments under a scanning electron microscope and X-ray energy spectroscope.

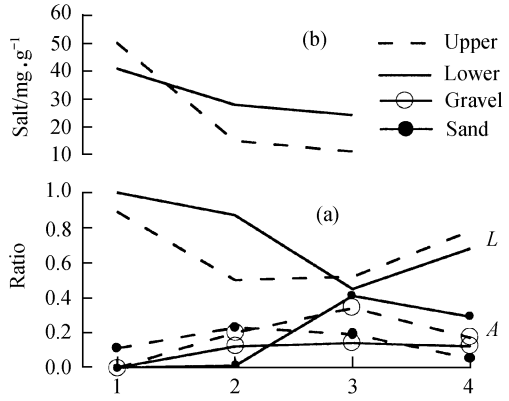


Fig. 1. Variations of *A/L* ratio (a) and average salt content (b). Profiles: 1, Jingerwa; 2, Xueergou; 3, Hongya; 4, Pulu.

### 3.1 Short-distance photography

In thin sections and short-distance photographs, we have observed the laminae in lower member along the Xueergou and Jingerwa profiles. They exhibit typical sedimentary ribbon-laminar texture and consist of dark- and light-color laminae alternatively. After an interval of tens of pairs of the dark- and light-color laminae a thick light-color lamina consisting of Ostracoda relicts and silt appears (fig. 2(a)). Gypsum lamella appears at the top of dark-color lamina below light-color lamina and represents a dry season. Every lamina is 0.3—1.5 mm thick. Bedding is mainly horizontally parallel (fig. 2(a)). There is also cross-bedding consisting of pure silt (fig. 2(b)), reflecting a disturbance by occasional inflow into the lake. Moreover, microripple was found (fig. 2(c)). Its wave peak is 0.2 cm and length –2 cm, with gentle front slope, about 5° , and steep rear slope, up to 18° , but no oblique bedding was observed on the section across wave peak line, resulting from wave process.

### 3.2 Observation under the scanning electron microscope

Under a scanning electron microscope, the occurrence and crystalline forms of gypsum were observed. The gypsum is almost holocrystalline. The layering gypsum is in the form of sheets of tabular crystals (fig. 2(d)). Locally swallow-tail twin appears (fig. 2(e)). The lamellar gypsum represents aggregate of acicular gypsum (fig. 2(f)) and aggregate of gypsum grains and sheets in druse. Tabular, sheet, and fibrous gypsum are achromatic, transparent selenite.

The occurrence forms of gypsum in laminae are: (i) gypsum microlamellae form a part of group of laminae; (ii) covering sand grains; (iii) filling pores; (iv) grained gypsum and druse attached to pore wall. The former three forms are primary sedimentary gypsum. The fourth is parasyngenetically crystallized gypsum rather than post-sedimentary filling material, since no melting or precipitation exist in its upper and lower laminae. It must be formed synchronously with the sedimentary lamina covering the top surface of crack.

### 3.3 Analysis on X-ray energy spectroscope

For testing the result of morphological observation under a scanning electron microscope, an analysis of the occurrence forms of gypsum was made on an X-ray energy spectroscope. The result shows that weight percents of S and Ca in lamellae containing gypsum are high, close to

atomic precent, and apparently different from the high Si content in its upper and lower sedimentary lamellae (table 2). The atomic percent of gypsum laminae is related to the gypsum occurrence form and content.

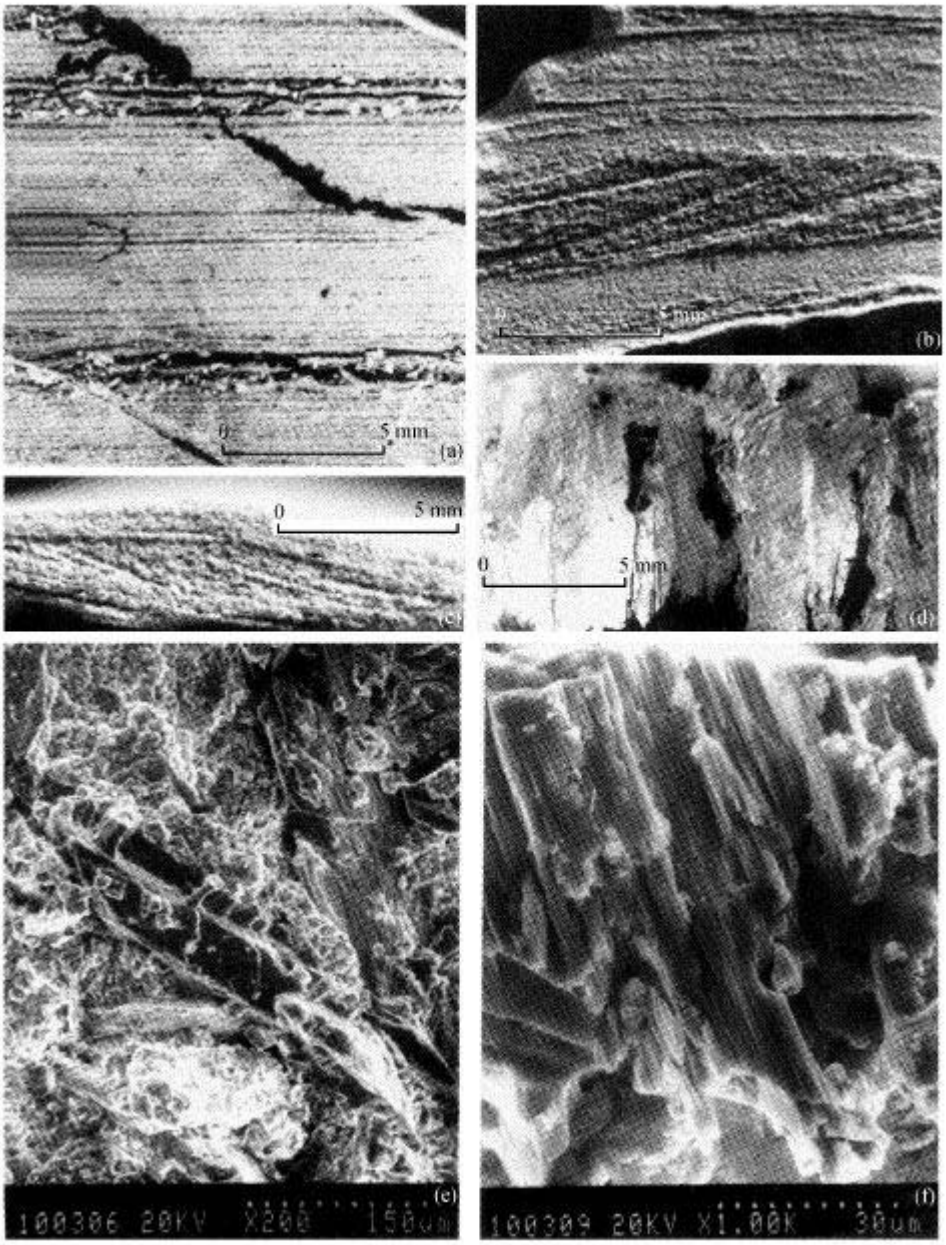


Fig. 2. (a) Laminae in shallow-lake deposit along the Jingerwa profile; (b) cross-bedding in shallow-lake deposit along the Jingerwa profile; (c) micro-ripples in shallow-lake deposit along the Jingerwa profile; (d) gypsum in lake-shore deposit along the Pulu profile; (e) swallow-tail twins in gypsum laminae; (f) gypsum laminae in deposit along the Jingerwa profile observed under a scanning electron microscope.

Table 2 Result of analysis on an X-ray energy spectroscope

| | Weight percent | | | | Atomic percent | | | |
|---|---|---|---|---|---|---|---|---|
| | Tabular gyps lamella | Upper sed. lamina | Gyps lamina | Lower sed. lamina | Tabular gyps lamella | Upper sed. lamina | Gyps lamina | Lower sed. lamina |
| Na | | 1.45 | 1.80 | 1.00 | | 1.39 | 1.74 | 1.71 |
| Mg | | 6.18 | 2.21 | 4.68 | | 5.61 | 2.10 | 4.20 |
| Al | | 5.90 | 2.85 | 7.79 | | 5.64 | 2.34 | 6.29 |
| Si | 0.58 | 19.87 | 7.07 | 22.47 | 0.47 | 15.61 | 5.58 | 17.43 |
| S | 23.59 | 1.54 | 16.54 | 1.34 | 16.62 | 1.06 | 11.43 | 0.90 |
| K | | 2.37 | 0.82 | 2.51 | | 1.34 | 0.46 | 1.40 |
| Ca | 28.48 | 13.54 | 20.54 | 8.00 | 16.06 | 7.51 | 11.08 | 4.95 |
| Fe | | 4.53 | 2.04 | 5.70 | | 1.79 | 0.81 | 2.22 |
| O | 47.34 | 43.52 | 45.54 | 44.77 | 66.86 | 60.04 | 64.46 | 60.98 |

## 4 Chemical analysis

According to the principle of 2 m equal-spacing and added sampling of varied layers, we collected sediment samples along three profiles and then analyzed soluble salt.

### 4.1 Soluble salt in shallow-lake deposit

The shallow-lake deposit, as shown along the Jingerwa profile, is clearly divided into two members from ion content in soluble salt. $Cl^-$ content in the upper member (0.40—24.22 m) along the profile is 4.69 times higher than that in the lower member. The distribution of $SO_4^{2-}$ is the opposite. Average $SO_4^{2-}$ content in the lower member is 3.57 times higher than that in the upper member. Thus, $SO_4^{2-}/Cl^{-1}<1$ in the upper member and >1 in the lower member. Cations $K^+$+$Na^+$ are predominant in the upper member and 4.16 times higher than in the lower member along the profile. Average $Ca^{2+}$ and $Mg^{2+}$ contents in the lower member are 3.76 and 3.20 times higher than those, respectively, in the upper member. Thus, $(K^+ + Na^+)/(Ca^{2+} + Mg^{2+})>1$ in the upper member and <1 in the lower member. If the sum of 8 major ions is representative of soluble salt content in lacustrine deposit, then the average soluble salt is 50.3 mg/g in the upper member of the deposit and 41.0 mg/g in the lower member.

The distribution of soluble salt ions along the Xueergou profile is that average $Cl^-$ content is still 3.28 times in the upper member higher than that in the lower member (table 3). $SO_4^{2-}$ content is 4.08 times in the lower member higher than that in the upper member. The distribution of $K^+$+$Na^+$, $Ca^{2+}$, and $Mg^{2+}$ is similar to that along the Jingerwa profile, but contents of all ions are lower than those along the Jingerwa profile. Therefore, average soluble salt content is 14.9 mg/g in the upper member and 27.9 mg/g in the lower member. From sedimentary records, the existence of multiple thin sand layers and multiple gravel layers in the upper and lower members along the Xueergou profile indicates that the effect of fresh water entering the lake may be the main cause for decreasing contents of various ions and average soluble salt content in the deposit. The sedimentary records along the Jingerwa profile show no effect of fresh water entering the lake. Thus,

the distribution of soluble salt can be more representative of the accumulation and evolution of soluble salt in the paleolake (fig. 1(b)).

Table 3 Average contents of major ions and soluble salt along the studied profiles

| Profile | Member | $CO_3^{2-}$ | $HCO_3^-$ | $Cl^-$ | $SO_4^{2-}$ | $K^++Na^+$ | $Ca^{2+}$ | $Mg^{2+}$ | Salt |
|---|---|---|---|---|---|---|---|---|---|
| Jingerwa | Upper | 5.45 | 2.15 | 134.63 | 26.95 | 141.45 | 12.74 | 15.05 | 50.3 |
| | Lower | 2.34 | 2.87 | 28.69 | 96.13 | 33.99 | 47.85 | 48.16 | 41.0 |
| | Total | 3.42 | 2.62 | 65.54 | 72.07 | 71.37 | 35.63 | 36.64 | 44.3 |
| Xueergou | Upper | 4.5 | 5.42 | 15.00 | 20.20 | 35.37 | 6.00 | 3.20 | 14.9 |
| | Lower | 3.41 | 2.51 | 4.57 | 82.44 | 23.23 | 27.41 | 35.61 | 27.9 |
| | Total | 3.90 | 3.80 | 9.20 | 54.78 | 28.63 | 17.90 | 21.21 | 22.1 |
| Hongya | Upper | 7.09 | 5.30 | 11.40 | 10.35 | 25.87 | 4.62 | 3.60 | 11.0 |
| | Lower | 3.30 | 3.76 | 52.29 | 20.37 | 59.64 | 8.79 | 11.29 | 24.3 |
| | Total | 5.33 | 4.58 | 30.42 | 15.01 | 41.57 | 6.56 | 7.17 | 17.2 |
| Pulu | Lower | 2.90 | 3.29 | 19.43 | 32.01 | 26.00 | 15.57 | 16.08 | 17.9 |

Ion content is in mmol/L; content of bivalent ions is doubled; salt content is in mg/g.

## 4.2 Soluble salt in lake-shore deposit

The Hongya-Nangou profile is representative of the lake-shore deposit profiles. Average anion content in upper member along the profile, such as $CO_3^{2-}$ increases, $Cl^-$ is only 1/4.95 of that in the lower member, and distinctly different from that along the Jingerwa profile; $SO_4^{2-}$ is 1/1. 97 of that in the lower member of the profile and tends to be similar to that along the Xueergou and Jingerwa profiles. But its average content in the upper member is only 1/1.95 of that along the Xueergou profile and 1/2.6 of that along the Jingerwa profile, respectively; and that of the lower member is correspondingly 1/4.05 and 1/4.72, respectively. Average contents of $K^++Na^+$ ions in the upper member are also lower than those in the lower member; average contents of $Ca^{2+}$ and $Mg^{2+}$ ions are lower than those along the Xueergou and Jingerwa profiles, but have similar regularity to them, i.e. the average contents in the upper member are lower than those in the lower member along the profiles. Average soluble salt content is 11.0 mg/g in the upper member and 24.3 mg/g in the lower member along the Hongya profile, lower than those along the Xueergou profile.

Why are the contents of all ions low and why does abnormal distribution of $Cl^-$ and $K^++Na^+$ appear in the upper and lower members along the profiles? The reasons are: first, the Hongya profile lies in a paleolake-shore zone, where sediment grains are generally more coarse and hence less capable to absorb salt. The lower member along the profile is a lake-shore swamp deposit, which is easy to release $H_2S$ and hence the total amount of $SO_4^{2-}$ ions decreases. Moreover, the lake beach was exposed during dry seasons and strong evaporation caused salinization on the beach surface. But salt on the beach surface was washed during rain seasons and was brought into shallow and deep lake zones, where it was accumulated. The process was repeated from year to year and thus chlorine salt could not be accumulated and preserved *in-situ*. Second, it can be seen in comparison between cumulative ratios and average soluble salt contents (fig. 1) that the deposit

near the Hongya-Nangou profile was acted by both river and lake nearly half-and-half. Thus, dilution and transport of salt by fresh water into shallow lake zone cannot be neglected. A piece of indirect evidence for the phenomenon is the salt accumulation in the central lake zone along the Jingerwa profile. Wang et al. have revealed a similar effect of fluvial process on the distribution of elements in lacustrine deposit[19].

## 5 Discussion

### 5.1 The nature and evolution of the paleolake

First, result of chemical analysis indicates that: (i) The ions of soluble salt in the lower member along the Xueergou and Jingerwa profiles are mainly $SO_4^{2-}$, $Ca^{2+}$, and $Mg^{2+}$; (ii) contents of these three ions increase progressively, horizontally from the Hongya profile to the Xueergou and Jingerwa profiles; (iii) among the cations in the lower member along the Pulu and Hongya profiles, $K^+$+$Na^+$ content is higher than $Ca^{2+}$ and also higher than $Mg^{2+}$, while $Ca^{2+}$ +$Mg^{2+}$ content is higher than $K^+$+$Na^+$ along the Pulu profile, but lower than $K^+$+$Na^+$ along the Hongya profile; (iv) soluble salt content is highest (41.0 mg/g) in the lower member along the Jingerwa profile. It follows that soluble salt in Nihewan paleolake water reached a degree at which $SO_4^{2-}$, $Ca^{2+}$ and $Mg^{2+}$ are dominant during the deposition of the lower member. Stratigraphical and microscopic observations show that gypsum interlayers occurred partially in the lower member along the Pulu profile and mirabilite occurred locally in the lower member along the Hongya profile. Most of the submembers of the lower member along the profile across the deposit in shallow lake zone intercalates thin gypsum layers and lamellae. It can be judged that the paleolake water has reached not only a degree at which $SO_4^{2-}$, $Ca^{2+}$ and $Mg^{2+}$ are dominant, but also a level at which gypsum can be crystallized from the soluble salt in water of shallow lake zone during dry seasons. It implies that the paleolake was developed to a critical state, into carbonate lake and sulfate lake. Therefore, water in the paleolake was at least weak-saline to semi-saline during deposition of the lower member along the profile. Result of study on mollusk fossils in Nihewan beds by Huang and Guo[9] and conclusions of Wang et al. in study of foraminifera in the area[20] can verify this suggestion.

Chemical analysis result of the upper member deposit along all profiles shows that the variation of soluble salt in lake-shore deposit is most complex. It was affected by river flow and by annual and inter-annual fluctuations of lake water level, so it is difficult to reflect the nature and evolution of the paleolake. Thus, we can only use the analysis result of soluble salt in shallow-lake deposit to reflect the nature of the paleolake. During deposition of the upper member along the profiles, although the deposit near Pulu and Hongya was commonly affected by the lake surface extension and the connection between Yuxian and Nihewan paleolakes and the thickness of lacustrine deposit increased, the fluvial deposit was still thick and did not completely depart from the lake-shore zone. The upper member deposit along the Xueergou profile is fluvial and lacustrine

half-and-half and formed in the lake-shore zone. Therefore, the analysis result of soluble salt in the upper member (0.40—24.22 m) along the Jingerwa profile can be used in reconstruction of the nature and evolution of the paleolake. Among ions of soluble salt in the upper member along the Jingerwa profile, $Cl^-$ and $K^+$+$Na^+$ are the main components, $Cl^-$ content is 3.9 times higher than the sum of all the other three anions, and $K^+$+$Na^+$ content is 5.1 times higher than that of $Ca^{2+}$ + $Mg^{2+}$. It indicates that soluble salt in the lake water that changed from an environment with $SO_4^{2-}$-$Ca^{2+}$-$Mg^{2+}$ is dominant in an environment in which $Cl^-$-$K^+$-$Na^+$ is dominant, and average soluble salt content in the deposit increased from 41.0 mg/L in the lower member to 50.3 mg/L in the upper member. By their solubility, KCl, NaCl, and $MgCl_2$ are more capable to migrate than $CaSO_4$, $K_2SO_4$, and $Na_2SO_4$ and can be readily accumulated in intracontinental lakes. At that time the paleolake must be a semi-saline lake changing into a chloride lake. But no salt rock deposit was observed in the field work. Therefore, we infer that there was an uninterrupted accumulation of chlorine salt in the paleolake during this stage.

In the top part along the Hongya and Xueergou profiles, a fluvial gravel layer occurs. In the vast area of the Nihewan basin, no swamp deposit widely developed in vanishing stage of the paleolake was found, except lake-shore swamp deposit, while the top part of lacustrine deposit is suddenly covered with fluvial gravel layer. It indicates that the vanishing of the Nihewan paleolake is catastrophic.

It is known from the above analysis that the Nihewan paleolake was weak-saline-semi-saline in its early stage and semi-saline in its late stage. Theoretically this character is suitable for the intracontinental lakes and similar to that of Daihai, Huangqihai, and other intracontinental lakes on the Qinghai-Xizang Plateau.

### 5.2 Problem of stratigraphical correlation

The analysis described above indicates that the Quaternary Nihewan deposit is a suite of strata accumulated in a weak-saline-semi-saline and semi-saline lake basin environment. This specific depositional environment for the Nihewan beds was neglected by researches in previous studies. But they have divided the post-$N_2$ deposit formed in Nihewan lake-shore zone in the area into the upper and lower beds[1] based on the principle of litho-stratigraphical and paleontological stratification. The facies and lithological changes in the lake-shore zone are far more complex than those in shallow and deep lake zones. The division result of deposit in lake-shore zone is difficult to use in correlation with deposits in shallow and deep lake zones. Therefore, we postulate here that using the sedimentary environment and environmental change events, syngenetic minerals, and fauna and flora, and taking into account geochronological methods in an integrated correlation is a better approach to overcoming the difficulty in stratigraphical division and correlation.

In the Nihewan area, there exist syngenetic gypsum layers and *Lamprotula* fossil in the lower member of paleolake-shore deposit along the Pulu profile and mirabilite and *Lamprotula* fossil

also in the lower member of the lake-shore deposit along the Hongya-Nangou profile. The lower members along the two profiles were deposited at a similar lake environmental condition and hence are of synchronous deposit and can be correlated. The lower member along the Xueergou profile is located in a transition zone from lake shore to shallow lake zone. It contains also gypsum layer. The Jingerwa profile lies in an ancient shallow lake zone, where the lower member deposit is mainly laminar and intercalates many gypsum lamellae. It can be seen that the lower member deposits along the four profiles are synchronous sediments deposited at different positions of a unified sulfate paleolake environment. They can be correlated to each other (fig. 3). Result of chemical analysis supports this judgment that the Nihewan beds are divided into upper and lower members, the hydrochemical environment of the lake and the paleoclimate during their deposition reflected in the members were distinctly different. The result of this division and correlation is basically coincident with recent division of the Nihewan beds by Yuan et al. from paleomagnetic and sporo-pollen data[14]. The upper member determined here approximately corresponds to member III divided by them and the lower member to member II divided by them.

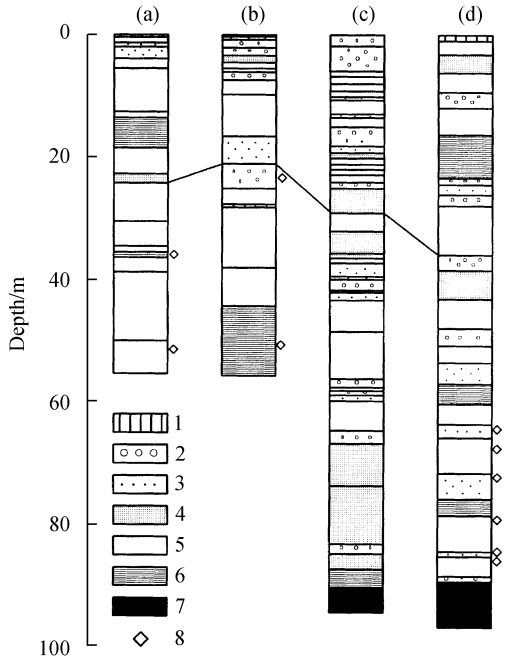


Fig. 3. Correlation between profiles. (a) Jingerwa; (b) Xueergou; (c) Hongya-Nangou; (d) Pulu. 1. Loess; 2, gravel; 3, sand; 4, silt; 5, clayey soil; 6, clay; 7, $N_2$ clay; 8, gypsum.

## 5.3 Environmental change

5.3.1 Paleoclimate environment. Intracontinental weak-saline-semi-saline lakes and semi-saline lakes show their evaporation exceeding precipitation recharge. Variation of evaporation and precipitation changes the constituent relation between $Cl^-$, $SO_4^{2-}$, $CO_3^{2-}$, $HCO_3^-$, $K^+$, $Na^+$, $Ca^{2+}$, and $Mg^{2+}$ and salt content[21]. This variation in Nihewan area is fairly clear (fig. 4). It reflects a change of relation between evaporation and recharge for the lake surface in semi-arid region.

The variation of soluble salt ions along the profiles shows that $CO_3^{2-}$ and $HCO_3^-$ are the slow ions to respond to climate change, except that along the Hongya profile on the lake shore. Variation of all ion contents along the profiles depends on the evolution stage of the lake. Lake water for lower member was of $SO_4^{2-}$-$Ca^{2+}$-$Mg^{2+}$ type. Thus, $SO_4^{2-}$, $Ca^{2+}$, and $Mg^{2+}$ contents vary significantly. The variation exhibits 5 peaks and 5 valleys and are coincident with that of soluble

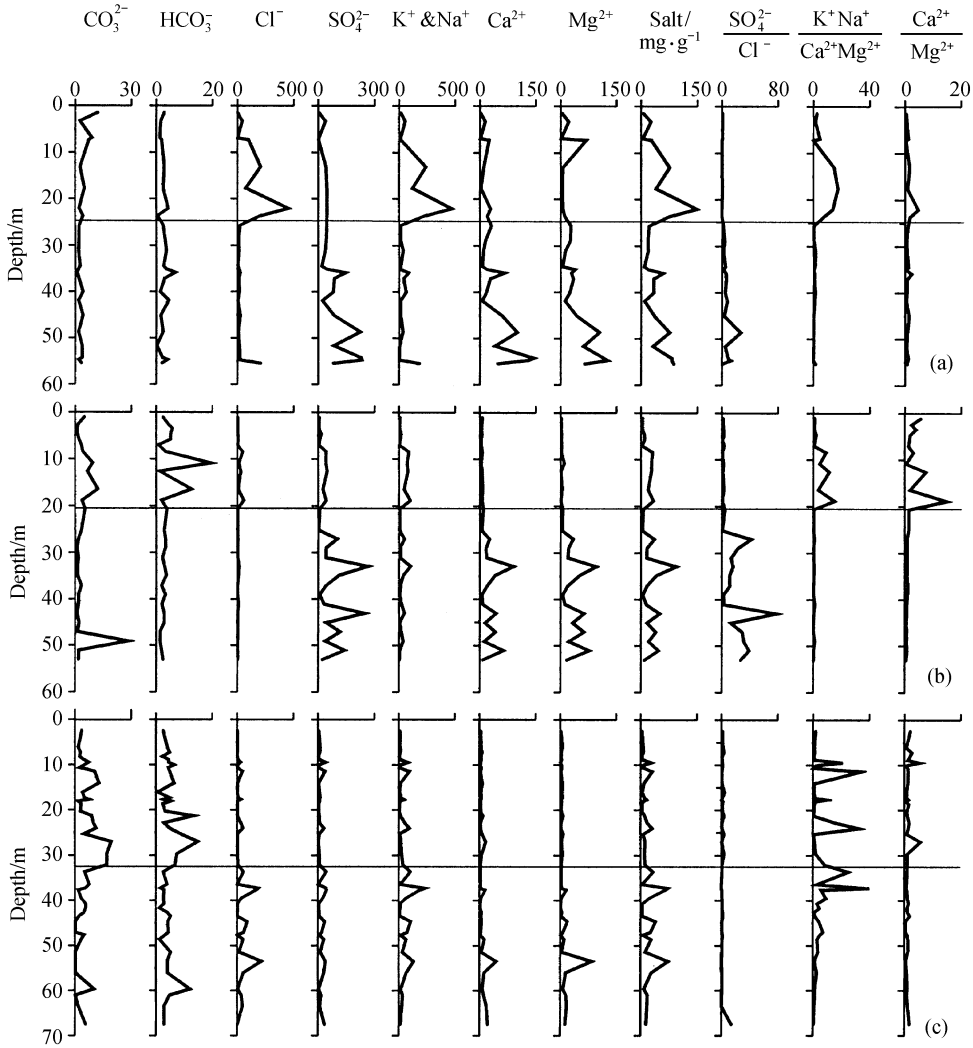


Fig. 4. Curves of major ions, soluble salt content, and ratios of ions along the profiles. (a) Jingerwa; (b) Xueergou; (c) Hongya-Nangou. Ion content is in mmol/L; content of bivalent ions is doubled.

salt content. Among the ratios of various ions, only $SO_4^{2-}/Cl^-$ varies similarly to $SO_4^{2-}$, $Ca^{2+}$, and $Mg^{2+}$. Their variation curves reflect clearly the climate change in Nihewan area during the deposition of lower member along the profiles. For the upper member along the profiles, lake water was either changing into or had become a $Cl^-$-$K^+$-$Na^+$ type water, indicating a further drought climate. At that time, $SO_4^{2-}$-$Ca^{2+}$-$Mg^{2+}$, and $SO_4^{2-}$/Cl did not significantly vary along the profiles. $Cl^-$, $K^+$+$Na^+$ and ($K^+$+$Na^+$)/($Ca^{2+}$+$Mg^{2+}$) variation curves reflect clearly the variation of precipitation in the area. Comparison of upper member with lower member shows that during deposition of the upper member it was drier with less precipitation. This is coincident with the

study result of Luochuan loess profiles. A study of Luochuan loess profiles by Liu Dongsheng et al. (1985) indicates that the average grain size of Lishi loess is larger than that of Wucheng loess; the average $CaCO_3$ content is higher than that of Wucheng loess; the relative accumulation degree of $SiO_2$, $Fe_2O_3$, and $Al_2O_3$ and the relative leaching degree of CaO in Wucheng loess are higher than those in Lishi loess; and $SiO_2/Al_2O_3$, $FeO/Fe_2O_3$, and CaO/ MgO ratios are lower than those in Lishi loess. It indicates that the climate during accumulation of Lishi loess was more dry than that during accumulation of Wucheng loess, resulting in strengthening winter wind and larger extent of Lishi loess accumulation than that of Wucheng loess[22]. The main body of Nihewan beds is of the lower Pleistocene. Therefore, the lower member along all profiles corresponds to the stage of Wucheng loess accumulation and the upper member to the early and middle stages of Lishi loess accumulation.

The variation curves of soluble salt in the lower member along all profiles exhibit 5 peaks and 5 valleys, reflecting 5 climate change cycles with dry and humid stages in the paleoclimate change. The peak values appear at drought stages and the valley values at humid stages with relative increasing precipitation. There were two short stages at which lake water was desalinized in the upper part of the lower member along the Hongya profile and the reciprocal first desalinization stage possibly lasted slightly longer (fig. 4). At that time the lake water was desalinized and became fresh water. Because the lake-shore is a place of river and lake interaction, it is more sensitive to environmental change than shallow lake zone.

As to the variation of soluble salt content in the upper member along the profiles, the upper member along the Hongya profile is characterized by 4 peaks and 5 valleys. The variation amplitude along the Xueergou and Jingerwa profiles is slightly larger, but with low frequency. Only 3—4 cycles were found. The reason may be that the upper member along the two profiles was in a zone, where chlorine salt easy to migrate was accumulated, and was related with its late accumulation.

5.3.2 Neotectonic movement. As the lower member changed into the upper member, the lake depth and its surface extent started to change. The boundary site of this change is near Hongya (see fig. 1). To the east and south of the boundary site, the lake was deepened and the surface extended. The lake-shore deposit is covered with thicker lacustrine deposit. To the north and west of the boundary site, lake water was shallowed, resulting in lacustrine deposit covered with stream-carried gravel layer, so that the shallow-lake cumulate of the lower member along the Xueergou profile changed into lake-shore cumulate of the upper member. This change is clearly shown at different positions of the same lake at the same time and may result from the neotectonic movement. That is, the lake bottom has rised up from Hongya to Xueergou, even further west. It led the lake water to be shallower in the west and north. This neotectonic movement started to occur approximately at the end of early Pleistocene and the beginning of middle Pleistocene and was synchronous with the uplift of Qinghai-Xizang plateau.

5.3.3 Evolution of the ancient water system. The intracontinental lakes are characterized by weak-saline to saline water. Sanggan River runs through the area and flows out from Shixia at the southeastern corner of Nihewan basin. A phase correlation between terraces led to suggest that the river had run across the Shixia at the beginning of middle Pleistocene[23]. However, the correlation between long-distance terraces could not be reliable because of lack of material correlation. As described above, since the Nihewan paleolake was an intracontinental weak-saline-semi-saline lake in its early stage and also an intracontinental semi-saline lake, the Sanggan River was an inflow stream which must rather flow into Nihewan lake basin when the paleolake exists than ran across the lake basin. The water system around the lake basin was not like the recent streams flowing into the Sanggan River. Most of the streams were independent, inflow streams into the lake basin. But the upstream branches of the Sanggan River flowed together through the master Sanggan River into the lake basin.

As for the cause for Sanggan River cutting through the Shixia, there may be three possibilities: (i) Neotectonic uplifting of lake basin bottom has caused the lake water to suddenly overflow the Shixia and cut a canyon. This suggestion is based on an uplift trace of the basin bottom found between Hongya and Xueergou. (ii) Catastrophic rain storm made the lake water level suddenly rise up and overflow through the Shixia. This suggestions is based on a thick fluvial gravel layer found at the top along the Hongya and Xueergou profiles. (iii) Headward erosion of lower river reaches. As the Shixia was cut through, the Nihewan paleolake was discharged and then vanished.

**Acknowledgements** The authors cordially thank Prof. Liu Zengsen for his participation in field investigation and sample collection and completion of chemical analysis of all samples. This work was supported by the National Natural Science Foundation of China (Grant No. 49471067).

## References

1. Barbour, G. B., Preliminary observations in the Kalgan Area, Bull. Geol. Soc. China, 1924, 3(2): 153.
2. Barbour, G. B., Licent, E., Teilhard de Chardin, P., Geological study of the deposits of the Sang Kan Ho Basin, Bull. Geol. Soc. China, 1927, 5(3-4): 263.
3. Teilhard de Chardin, P., Piveteau, J., The mammal fossils of Nihowan (China), Annales de Paleontologie (in French), 1930, 19: 3.
4. Black, D., Teilhard de Chardin, P., Young, C. C. et al., Fossil man in China, Mon. Geol. Surv. China, Ser. A, 1933, (11): 1.
5. Young, C. C. , The boundary between Pliocene and Pleistocene, Science (in Chinese), 1949, 31(11): 332.
6. Gai, P., Wei, Q., Discovery of a stone artifact from Lower Pleistocene, Nihowan, Vertebrata Palasiatica (in Chinese), 1974, 12(1): 69.
7. Chia, L. P. , Wei, Q. , Li, C. R. , Report on the excavation of Hsuchiayao Man Site in 1976, Vertebrata Palasiatica (in Chinese), 1979, 17(4): 288.
8. You, Y. Z., New materials from Xiaochangliang Paleolithic Site, Hebei Province, and the problem of its date (in Chinese), Prehistoric Research, 1983, (1): 46.
9. Huang, B. Y. , Guo, S. Y. , Discussion on stratigraphic division, geological period and palaeography of the Nihewan according to the Mollusca, Bulletin of the Tianjin Institute of Geology and Mineral Resources, Chinese Academy of Geological Sciences (in Chinese), 1981(4): 17.
10. Cheng, G. L. , Lin, J. L. , Li, S. L. et al., A preliminary paleomagnetic survey of the Nihewan Bed, Scientia Geologica Sinica (in Chinese), 1978(3): 247.
11. Li, H. M. , Wang, J. D. , Magnetostratigraphic study of Nihewan Formation, Annual Reports of Institute of Geochemis-

try(1982-1983) (in Chinese), Guiyang: Guizhou People' s Publishing House, 1983, 182—184.

12. Li, R. Q. , Yuan, B. Y. , Discovery of Pleistocene stromatolites in Nihewan Area, Hebei Province, Scientia Geologica Sinica (in Chinese), 1992, (1): 97.
13. Xia, Z. K. , Zhang, Y. , Yang, D. J. et al., Stromatolites discovered in Nihewan Formation and their paleoenvironment, Science in China, Ser. B, 1994, 37(5): 634.
14. Yuan, B. Y. , Zhu, R. X. , Tian, W. L. et al., The age, stratigraphic classification and correlation of the Nihewan Formation, Science in China (in Chinese), Ser. D, 1996, 26(1): 67.
15. Cao, J. X. , Neotectonic movements and volcanic activities in the southeast of Datong Basin (Shanxi), China Quaternary Research (in Chinese), 1959, 2(2): 60.
16. Yang, J. C. , Geomorphology and Quaternary geology in the east of Datong Basin, ACTA Scientiarum Naturalium University Pekinensis (in Russian), 1961, 7(1): 87.
17. Zhou, T. R. , Li, H. Z. , Liu, Q. S. et al., Cenozoic Palaeogeography of the Nihewan Basin (in Chinese), Beijing: Science Press, 1991, 1—162.
18. Chen, M. N. (editor-in-chief), Study on the Nihewan Beds (in Chinese), Beijing: China Ocean Press, 1988, 1—145.
19. Wang, S. M., Yu, Y. S., Wu, R. J. et al., Lake Daihai: Lacustrine Environment and Climatic Changes (in Chinese), Hefei: Publishing House of China University of Science and Technology, 1990, 1—191.
20. Wang, P. X. , Min, Q. B. , Lin, J. X. et al., The discovery of semi-saline foraminiferal fossil faunas from Cenozoic basins in the east of China and their significance, Contribution to Strati-paleontology (in Chinese), 1975(2): 1.
21. Luckaschev, K. I. , Luckaschev, V. K. , Geochemistry of Hypergene Zone (translated into Chinese by Zeng Zhiyuan), Beijing: Scientific and Technological Literature Press, 1992, 1—237.
22. Liu, T. S., Loess and Environment (in Chinese), Beijing: Science Press, 1985, 191—302.
23. Song, J. S., Wang, X. Y. , Geomorphologic analysis of the Sangganhe Gorge at Shixiali in the Nihewan Basin, in Proceedings of the 3rd Symposium on Quaternary in China (in Chinese), Beijing: Science Press, 1982, 311.